Human Molecular Genetics, 2019, Vol. 29, No. 4 591–604

doi: 10.1093/hmg/ddz278
Advance Access Publication Date: 9 December 2019
General Article

GENERAL ARTICLE

The master transcription factor SOX2, mutated in anophthalmia/microphthalmia, is post-transcriptionally regulated by the conserved RNA-binding protein RBM24 in vertebrate eye development

Soma Dash[1], Lindy K. Brastrom[2], Shaili D. Patel[1], C. Anthony Scott[2,3], Diane C. Slusarski[2] and Salil A. Lachke[1,4,*]

[1]Department of Biological Sciences, University of Delaware, Newark, DE 19716 USA, [2]Department of Biology, University of Iowa, Iowa City, IA 52242 USA, [3]Department of Pediatrics, Baylor College of Medicine, Houston, TX, 77030, USA and [4]Center for Bioinformatics and Computational Biology, University of Delaware, Newark, DE 19716 USA

*To whom correspondence should be addressed at: Department of Biological Sciences, University of Delaware, Newark, DE 19716, USA. Tel: +302-381-3040; Fax: +302-831-2281; Email: salil@udel.edu

Abstract

Mutations in the key transcription factor, SOX2, alone account for 20% of anophthalmia (no eye) and microphthalmia (small eye) birth defects in humans—yet its regulation is not well understood, especially on the post-transcription level. We report the unprecedented finding that the conserved RNA-binding motif protein, RBM24, positively controls Sox2 mRNA stability and is necessary for optimal SOX2 mRNA and protein levels in development, perturbation of which causes ocular defects, including microphthalmia and anophthalmia. RNA immunoprecipitation assay indicates that RBM24 protein interacts with Sox2 mRNA in mouse embryonic eye tissue. and electrophoretic mobility shift assay shows that RBM24 directly binds to the Sox2 mRNA 3'UTR, which is dependent on AU-rich elements (ARE) present in the Sox2 mRNA 3'UTR. Further, we demonstrate that Sox2 3'UTR AREs are necessary for RBM24-based elevation of Sox2 mRNA half-life. We find that this novel RBM24–Sox2 regulatory module is essential for early eye development in vertebrates. We show that *Rbm24*-targeted deletion using a constitutive CMV-driven Cre in mouse, and *rbm24a*-CRISPR/Cas9-targeted mutation or morpholino knockdown in zebrafish, results in Sox2 downregulation and causes the developmental defects anophthalmia or microphthalmia, similar to human SOX2-deficiency defects. We further show that Rbm24 deficiency leads to apoptotic defects in mouse ocular tissue and downregulation of eye development markers Lhx2, Pax6, Jag1, E-cadherin and gamma-crystallins. These data highlight the exquisite specificity that conserved RNA-binding proteins like RBM24 mediate in the post-transcriptional control of key transcription factors, namely, SOX2, associated with organogenesis and human developmental defects.

Received: August 26, 2019. **Revised:** October 24, 2019. **Accepted:** November 10, 2019

Introduction

Several key transcription factors, including LHX2, OTX2, PAX6, RAX, SIX3, SIX6 and SOX2, among others, are involved in early stages of vertebrate eye development, in the specification of an eye field in the anterior neural plate (1–3). Subsequently, Sonic hedgehog signaling bifurcates the single eye field into two structures termed optic sulci that interact with their opposing surface ectoderm tissue, to eventually form the retina and lens, respectively (4). Thus far, precise spatiotemporal expression of key transcription and signaling factors are shown to be necessary for these processes, disruption of which causes developmental ocular defects.

Indeed, developmental eye disorders such as microphthalmia (small eye) and anophthalmia (no eye) affect 1 in 7000 and 1 in 30 000 live human births, respectively (5,6). About 20% of human anophthalmic cases are linked to mutations in the *SOX2* gene alone, which, in addition to its critical function in development of eye (7–9) and other organs, is also one of the Yamanaka cellular reprogramming factors that controls pluripotency (9–12). While transcriptional regulation of *Sox2* is characterized in detail in various developing tissues (13), the impact of post-transcriptional regulatory mechanisms, particularly those regulated by RNA-binding proteins (RBPs), on the fate of its transcribed mRNA is less clear. This reflects a larger knowledge gap, as there are similar numbers of transcription factors and RBPs encoded by the human genome, but the functional significance of the latter in development is not well described (14–17).

We recently published an update to the database 'iSyTE' (integrated Systems Tool for Eye gene discovery) which allows *in silico* prediction of genes linked to eye development and disease (18–20). However, such iSyTE gene predictions need to be tested experimentally to conclusively establish their role in eye development and disease. Here, we applied iSyTE to identify a new regulator of eye development—the RNA-binding motif family protein, RBM24. RBM24 is a highly conserved RBP in vertebrates with a single RNA recognition motif domain located near its N-terminus (21,22). Thus far, RBM24 has been largely studied in the context of alternative splicing in cardiac development and differentiation (23–25). Further, RBM24 has been implicated in controlling mRNA decay of the cell cycle regulators p63 and p21 and the mRNA stability of the myogenic factor MyoD and translation of p53 (26–28).

Here we report the unprecedented finding that RBM24 binds to the AU-rich elements (AREs) within the 3'UTR of *Sox2* mRNA and leads to its stabilization, which is necessary for normal expression levels of SOX2 protein in eye development. We find that *Rbm24* deficiency in mouse and fish results in downregulation of Sox2 and causes the eye defects anophthalmia and microphthalmia. *Rbm24* knockout mice show elevated apoptosis in developing ocular tissue and abnormal expression of eye development regulators and markers such as LHX2, PAX6, JAG1, E-cadherin and γ-crystallin. These data provide a transformational understanding of RBP-mediated post-transcriptional control of key transcriptional regulators, particularly SOX2, in organogenesis.

Results

RBM24 deficiency causes microphthalmia and anophthalmia in mouse

Using the bioinformatics tool iSyTE (integrated Systems Tool for Eye gene discovery), which prioritizes genes based on eye tissue enrichment scores (18–20,29–32), we identified Rbm24 as a potential regulator of eye development (Fig. 1A). In mouse, RBM24 is expressed in the presumptive lens ectoderm and the optic vesicle at embryonic day (E) 9.5 (33) (Fig. 1B) and later in the lens and the retina (Fig. 1C), suggesting that RBM24 functions in eye development from early stages.

To investigate RBM24 function in development, we generated a new *Rbm24* constitutive knockout mouse line, *Rbm24*$^{-/-}$, and confirmed the absence of RBM24 at both RNA and protein levels in mutant tissue (Fig. 1D-H). *Rbm24*$^{-/-}$ mice die at variable frequency after E7.5 and do not survive after E14.5, and further, after stage E9.5, they are smaller in contrast to control (Table 1). The embryonic lethality defect is observed in an independently generated *Rbm24* null mouse line and is attributed to cardiac abnormalities (23).

Here, we demonstrate that both *Rbm24*$^{-/-}$ mice exhibit severe ocular defects at 100% penetrance. At E11.5, approximately half of the *Rbm24*$^{-/-}$ mice exhibit anophthalmia (absent/rudimentary ocular tissue due to arrested eye development) on one side and microphthalmia (small eye) on the other, while the remainder of the mutants exhibit bilateral microphthalmia (Fig. 2A-D').

rbm24a deficiency causes eye defects in zebrafish

Zebrafish have two *Rbm24* orthologs (*rbm24a* and *rbm24b*), and we examined the expression of both orthologs by *in situ* hybridization (ISH). *rbm24a* is expressed early in the eye, heart and somites (Fig. 3A). And, analogous to mouse, *rbm24a* becomes enriched in the lens at 2-day post fertilization (dpf) (Fig. 3B). In contrast, *rbm24b* exhibits high expression in the heart and somites with little or no expression in the developing eye tissue (Fig. 3C, C'). The expression patterns of *rbm24a* and *rbm24b* are supported by the zebrafish single-cell RNA sequencing database, SPRING (34). Additionally, we previously demonstrated that *rbm24a* morphant zebrafish have visual defects (35). These data suggest that *rbm24a* likely functions in the eye, and therefore we used morpholinos and CRISPR/Cas9 to generate *rbm24a* knockdown and deletion, respectively, in zebrafish. In a dose-dependent manner, *rbm24a* morphants exhibit progressively severe microphthalmia at high frequency (1 ng, 76%; 2 ng, 92%) or anophthalmia (rudimentary or diffused ocular tissue) at 1.5% penetrance at 3 dpf stage (Fig. 3D-E', Table 2). To confirm the zebrafish *rbm24a* knockdown phenotypes, CRISPR/Cas9 was used to generate deletions in *rbm24a*, which resulted in microphthalmia in F0 embryos at 3 dpf stage (Fig. 3F-G').

Together, these data identify RBM24 as a new post-transcriptional regulator necessary for eye development in vertebrates.

Rbm24-deficient mouse eye tissue exhibits apoptotic defects

Because microphthalmia/anophthalmia can result from elevated apoptosis in development (36–38), we performed cell death analysis, which demonstrated *Rbm24*$^{-/-}$ ocular tissue to have high number of TUNEL-positive cells (Fig. 4A-E). We find that the Notch pathway effector JAG1, which positively controls apoptosis inhibitors and functions in eye development (39,40), is downregulated at both the mRNA and protein levels in *Rbm24*$^{-/-}$ mice (Fig. 4F-H). These data suggest that RBM24-mediated positive control of JAG1 is necessary for cell viability in eye development and the disruption of this regulatory module contributes to the pathology of the ocular defects in *Rbm24* mutants. Further, one of the apoptosis inhibitors

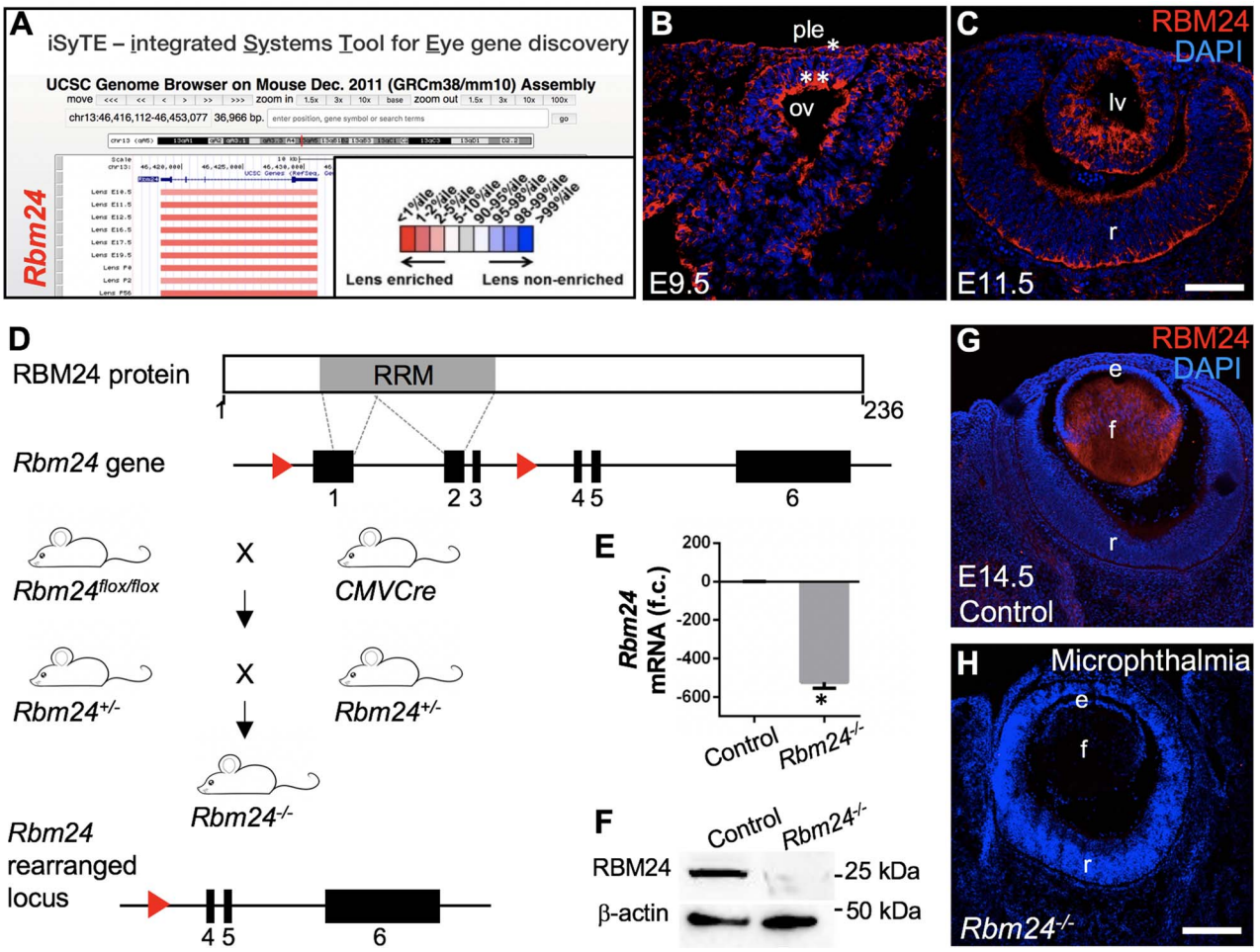

Figure 1. RBM24 is expressed during mouse eye development. (**A**) iSyTE prioritizes *Rbm24* as a gene with potential function in the eye based on high lens-enriched expression. Heat map red intensity indicates high lens enrichment. (**B**) During mouse development, Rbm24 protein is expressed in the presumptive lens ectoderm (*) and optic vesicle (**) at embryonic day (E)9.5 and (**C**) in the cornea, lens anterior epithelial cells and fiber cells at E14.5. (**D**) Generation of *Rbm24*$^{-/-}$ mice using floxed *Rbm24* alleles and CMV promoter-driven Cre recombinase. (**E**) RT-qPCR demonstrates *Rbm24* downregulation in *Rbm24*$^{-/-}$ embryos at E7.5. (**F**) Western blot analysis confirms absence of RBM24 protein in *Rbm24*$^{-/-}$ mouse embryonic tissue at E14.5. (**G, H**) Immunostaining shows absence of Rbm24 protein in *Rbm24*$^{-/-}$ mouse eye tissue at E14.5. Abbr.: ple, presumptive lens ectoderm; ov, optic vesicle; e, anterior lens epithelium; f, lens fiber cells; r, retina; f.c., fold change. Asterisks in E indicate *P*-value < 0.005. Scale bar for B, C, J, K is 70 µm, for G, H is 140 µm.

Table 1. Embryonic lethality and ocular defects in *Rbm24*$^{-/-}$ mice

Embryonic stage	Number of litters dissected	Number of litters with no *Rbm24*$^{-/-}$ embryos	Number of *Rbm24*$^{-/-}$ embryos	Unilateral anophthalmia *Rbm24*$^{-/-}$ embryos	Bilateral microphthalmia *Rbm24*$^{-/-}$ embryos
E7.5	6	1	11	na	na
E9.5	12	5	14	na	na
E10.5	10	6	5	2	3
E11.5	5	2	6	3	3
E12.5	9	5	5	2	3
E14.5	7	4	6	2	4

regulated by JAG1, namely, BIRC2 (41), is severely downregulated in *Rbm24*$^{-/-}$ mouse ocular tissue at the mRNA level (Fig. 4I). Interestingly, RBM24 binds to *Birc2* mRNA directly as shown by RNA immunoprecipitation (RIP) assay suggesting that RBM24-mediated regulation of apoptotic inhibitor is required for cell viability in the ocular tissue (Fig. 4J).

RBM24 deficiency causes downregulation of key eye development markers

To gain further insight into the molecular basis of the ocular phenotype in *Rbm24*$^{-/-}$ mice, we examined the expression of lens development markers PAX6, E-cad (E-cadherin) and γ-cry

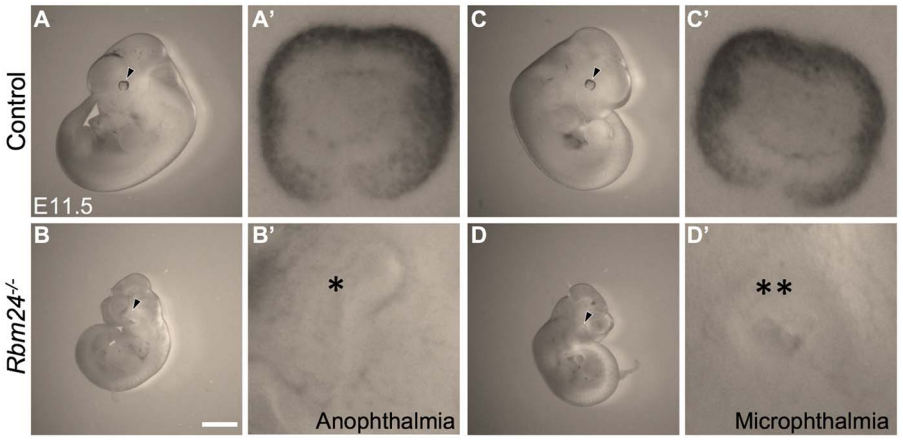

Figure 2. *Rbm24* is required for mouse eye development. (**A-D'**) At E11.5, *Rbm24*$^{-/-}$ mice exhibit anophthalmia (*) on one side and microphthalmia on the other side (**). Abbr.: l, lens; r, retina.

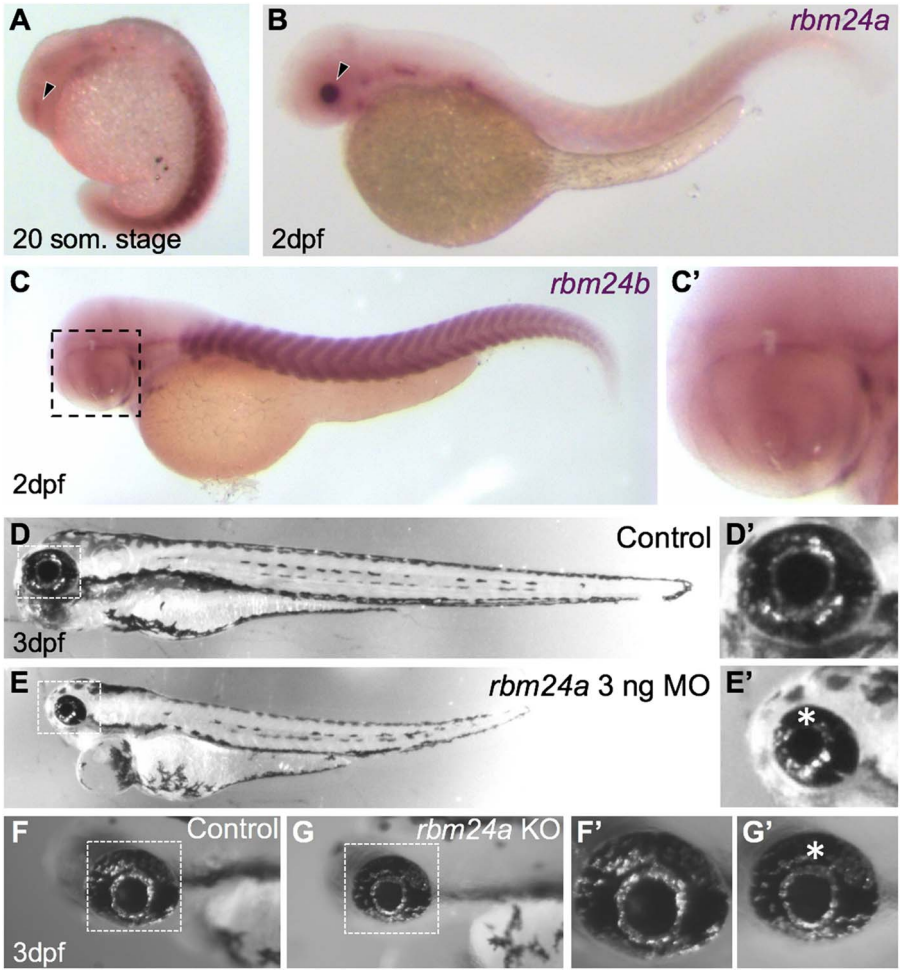

Figure 3. *rbm24a* is required for zebrafish eye development. (**A**) ISH shows *rbm24a* transcript expression in the eye (arrowhead), heart and somites at 20 somite stage (~19hpf). (**B**) At stage 2 dpf *rbm24a* transcript expression is strong in the eye region (arrowhead). (**C-C'**) At stage 2 dpf *rbm24b* transcript expression is expressed in the somites, but expression in the eye tissue is not detected. (**D-E'**) While control eyes are normal, *rbm24a* morpholino injected embryos exhibit microphthalmia (asterisk). (**F-G'**) CRISPR/Cas9-based targeted *rbm24a* deletion zebrafish exhibit microphthalmia (asterisk). Abbr.: MO, morpholino; KO, knockout; l, lens; r, retina.

(gamma-crystallins). In the mildly affected *Rbm24*$^{-/-}$ embryos, PAX6 is undetected in the anterior cells of the lens vesicle. Further, Pax6 was detectable in only a few cells in the posterior region of the lens vesicle. On the other hand, in the severely affected *Rbm24*$^{-/-}$ embryos, PAX6 is undetected in the region where lens vesicle is normally formed. Pax6 expression in the retina of *Rbm24*$^{-/-}$ embryos is unaltered (Fig. 5A-C). While E-cad and γ-cry are significantly reduced in less-severely affected

Table 2. Ocular defects in *rbm24a* morphant and F01 mutant zebrafish

Treatment	Microphthalmia/anophthalmia	Normal	Total
Uninjected	1/0	220	221
Control MO (1–2 ng)	2/0	238	240
rbm24a AUG MO (1–1.5 ng)	109/0	32	141
rbm24a AUG MO (2–2.5 ng)	125/2	11	138
rbm24a F0 CRISPR injected	49/0	24	73

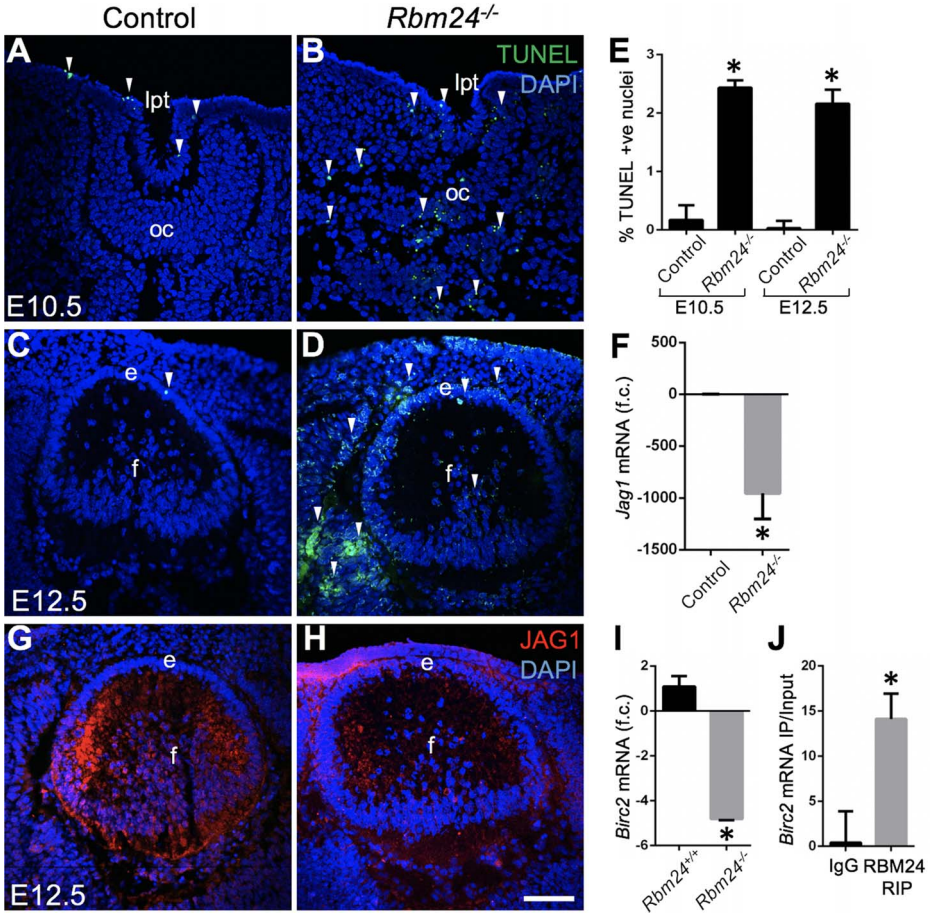

Figure 4. RBM24 deficiency causes apoptotic defects. (**A-D**) In contrast to control, *Rbm24*$^{-/-}$ mice have high number of TUNEL-positive nuclei (arrowhead) in the ocular region at E10.5 and E12.5. (**E**) Quantification of TUNEL immunofluorescence indicates significantly higher number of apoptotic nuclei in *Rbm24*$^{-/-}$ ocular region. (**F**) RT-qPCR analysis indicates significant Jag1 downregulation in *Rbm24*$^{-/-}$ in contrast to controls. (**G, H**) Immunostaining analysis indicates Jag1 is downregulated in E12.5 *Rbm24*$^{-/-}$ lenses in contrast to control. (**I**) RT-qPCR analysis indicates significant *Birc2* downregulation in *Rbm24*$^{-/-}$ in contrast to controls. (**J**) RNA immunoprecipitation with RBM24 antibody on mouse embryonic eye tissue shows enrichment of *Birc2* mRNA. Abbr.: lpt, lens pit; oc, optic cup; e, lens epithelial cells; f, lens fiber cells; r, retina; f.c., fold change. Asterisks in E, F, I, J indicate a P-value < 0.05. Scale bar for A-D, G, H is 70 µm; # indicates whole-body tissue.

mutant lenses, E-cad is downregulated, and γ-cry is absent in severely affected mutant lenses, suggesting abnormalities in lens epithelial and fiber cells, and therefore lens differentiation, in *Rbm24*$^{-/-}$ embryos (Fig. 5D-I).

Next, we investigated early eye development markers, namely, SOX2 and LHX2, which are linked to anophthalmia and/or microphthalmia.

LHX2 is a direct target of RBM24

Because Rbm24 is expressed in the optic vesicle, we next examined whether its deficiency impacted LHX2 expression. We find LHX2 is downregulated in the optic vesicle of *Rbm24*$^{-/-}$ mice at E9.5 (Fig. 6A and B) and consistently, *Lhx2* mRNA is severely downregulated in *Rbm24*$^{-/-}$ eye tissue (Fig. 6C). Furthermore, we performed RIP assay using Rbm24 antibody on E14.5 wild-type whole eye lysates and find enrichment of *Lhx2* mRNA in the Rbm24 antibody pulldown (Fig. 6D). As confirmation, we performed *Rbm24* knockdown in NIH3T3 cells and found significant downregulation of *Lhx2* mRNA (Fig. 6D). Further, *Lhx2* is significantly upregulated when RBM24 is overexpressed in 21EM15 lens epithelial cell lines (Fig. 6F). To address mRNA stability, 21EM15 cells transfected with the RBM24 overexpression vector were treated with the general transcriptional inhibitor actinomycin D, and the rate of *Lhx2* mRNA decay was measured. We observed an increase in the half-life of *Lhx2* transcript in

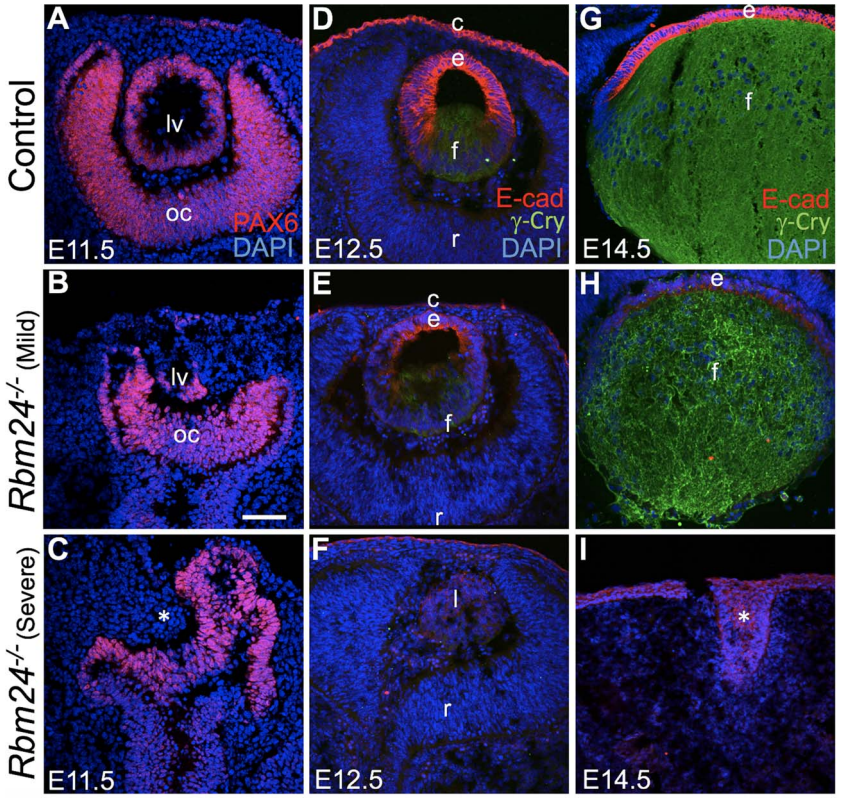

Figure 5. *Rbm24*$^{-/-}$ mice exhibit downregulation of eye development markers. (**A-C**) PAX6 is significantly downregulated in the lens vesicle, but not in the retina tissue of *Rbm24*$^{-/-}$ at E11.5 in contrast to control. (**D-I**) E-cad and gamma-cry are severely downregulated in lens epithelial and lens fiber cells, respectively, at E12.5 and E14.5 in *Rbm24*$^{-/-}$ in contrast to control. Abbr.: c, cornea; e, lens epithelial cells; f, lens fiber cells; l, lens; r, retina; se, surface ectoderm; ov, optic vesicle; lv, lens vesicle; oc, optic cup. Scale bar for A-I is 70 µm.

RBM24 overexpressing cells in contrast to the controls (Fig. 6G), indicating that RBM24 stabilizes *Lhx2* transcript.

SOX2 is a direct target of RBM24

Because, SOX2 is required for the sustained expression of PAX6 in early lens development (42) and is linked to human anophthalmia/microphthalmia, we next investigated the expression of SOX2 in *Rbm24*$^{-/-}$ mice. Interestingly, SOX2 protein is significantly downregulated in *Rbm24*$^{-/-}$ mice during early eye development at E9.5 in the presumptive lens ectoderm and optic vesicle (Fig. 7A-B') and is undetected in *Rbm24*$^{-/-}$ ocular tissue at later developmental stages (Fig. 7C-D'). *Sox2* mRNA is expectedly found to be severely downregulated in *Rbm24*$^{-/-}$ eye tissue (Fig. 7E). Moreover, *sox2* mRNA is also found to be downregulated in *rbm24a* morphants zebrafish (Fig. 7F), suggesting that the function of RBM24 in controlling SOX2 is conserved during development in vertebrates. Interestingly, *Sox2* mRNA 3'UTR has three AREs (henceforth referred as A1, A2 and A3) (Fig. 8A), which is significant because RBM24 can bind AREs in other mRNAs (namely, p21 and p63) in human colorectal carcinoma cells (26,27). Therefore, we hypothesized that RBM24 regulates *Sox2* mRNA through the AREs and first tested the possibility that RBM24 directly binds to *Sox2* ARE by performing electrophoretic mobility shift assay (EMSA). We find that the full-length RBM24 protein binds, in a sequence-specific manner, to a 20 bp biotin-labeled RNA oligomer that contains the *Sox2* 3'UTR ARE site A1, A2 and A3 (Fig. 8B-D). The RBM24 protein–*Sox2* 3'UTR RNA complex can be competed out with a 1000-fold excess of the non-biotinylated wild-type ARE oligomer, but not with the non-biotinylated mutant ARE oligomer (Fig. 8B-D). Furthermore, we performed RIP assay that shows enrichment of *Sox2* mRNA in the Rbm24 antibody pulldown (Fig. 8E). Together, these findings demonstrate that Rbm24 directly binds to *Sox2* mRNA through interaction with its 3'UTR ARE.

RBM24 positively controls Sox2 mRNA stability

To understand the biological significance of RBM24 binding with Sox2 mRNA, and thereby investigate the molecular mechanism by which it regulates SOX2 expression, we next performed reporter analysis. First, we confirmed that in NIH3T3 fibroblast cells, *Rbm24* knockdown using siRNA results in downregulation of *Sox2* mRNA similar to that of *Rbm24*$^{-/-}$ ocular tissue (Fig. 8F). We co-transfected NIH3T3 cells with an Rbm24 overexpression vector and a *Sox2* reporter vector, which carries the *Renilla luciferase* open reading frame (ORF) fused to *Sox2* 3'UTR. After treating co-transfected cells with actinomycin D, the rate of *luciferase* mRNA decay was measured. We find that RBM24 overexpression causes an increase in the half-life of luciferase–*Sox2* 3'UTR fusion reporter transcript (Fig. 8G), indicating that RBM24 stabilizes *Sox2* transcript through interactions with its 3'UTR. Next, we performed mRNA decay assay on RBM24 overexpressing NIH3T3 cells co-transfected with reporter vector wherein *luciferase* is fused with various mutated versions of *Sox2* 3'UTR. Unlike wild-type Sox2 3'UTR that contains intact ARE sites, mutation of the ARE sites A1, A2 or A3 individually, or all three sites concomitantly, did not result in a similar increase

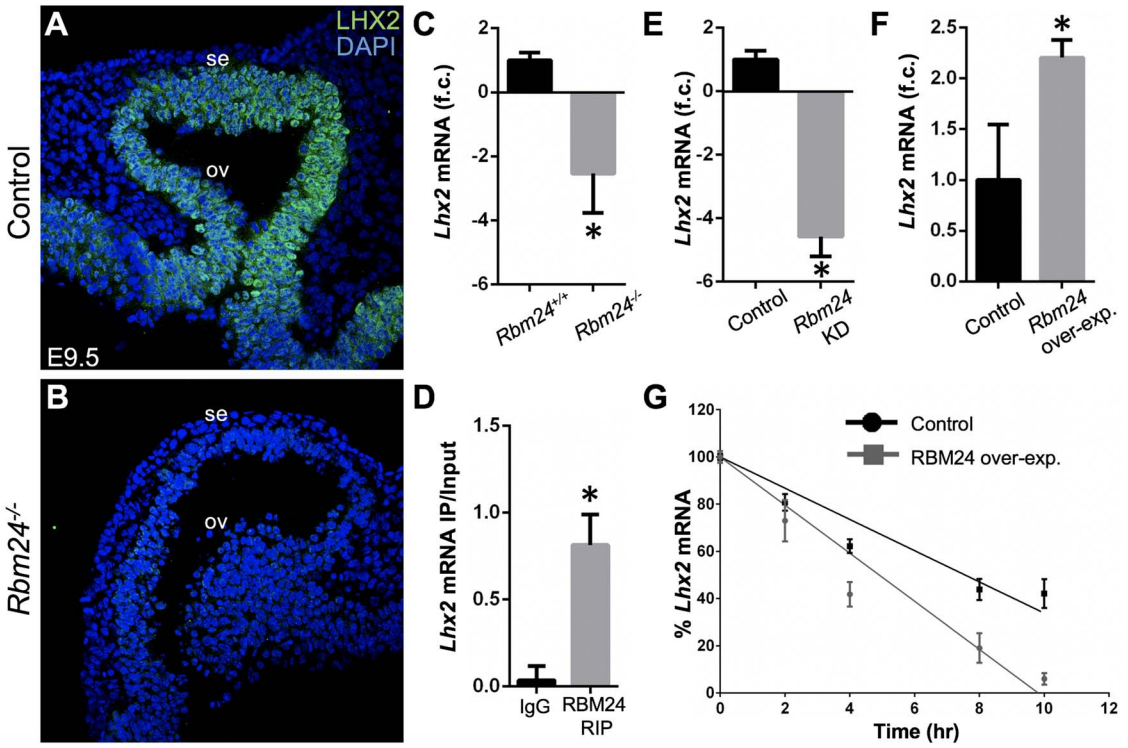

Figure 6. RBM24-deficient mouse exhibit downregulation of LHX2 expression. (**A, B**) Lhx2 is significantly downregulated in the optic vesicle of *Rbm24*$^{-/-}$ at E9.5 in contrast to control. (**C**) RT-qPCR analysis confirms significant *Lhx2* downregulation in *Rbm24*$^{-/-}$ mice. (**D**) RNA immunoprecipitation with Rbm24 antibody on mouse embryonic eye tissue shows enrichment of *Lhx2* mRNA. (**E**) *Rbm24* KD in NIH3T3 cells results in downregulation of *Lhx2* transcript. (**F**) Overexpression of Rbm24 in 21EM15 cells causes upregulation of *Lhx2* transcript. (**G**) Rbm24 overexpression in 21EM15 cells results in significant increase in the half-life of *Lhx2* mRNA. Abbr.: se, surface ectoderm; ov, optic vesicle; f.c., fold change. Asterisks in C-F indicate *P*-value < 0.05. Scale bar in A, B is 70 µm.

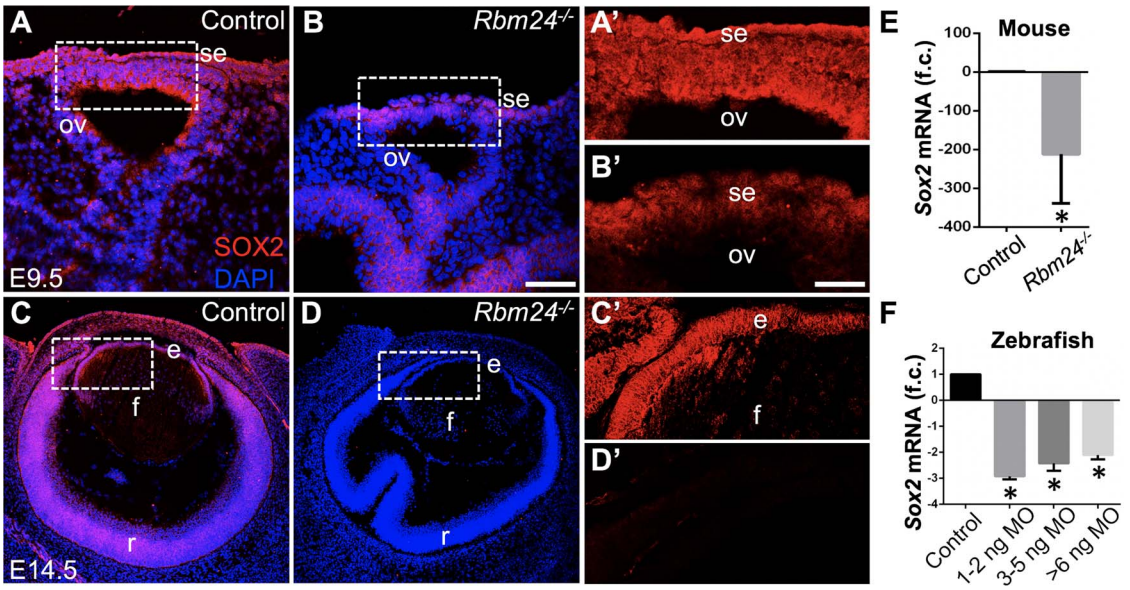

Figure 7. RBM24-deficient mouse and zebrafish exhibit downregulation of SOX2 expression. (**A-B'**) At early eye development stage E9.5, immunostaining shows that *Rbm24*$^{-/-}$ mice exhibit significant reduction of SOX2 protein in the surface ectoderm (future lens) and the optic vesicle (future retina). (**C-D'**) By E14.5, even the *Rbm24*$^{-/-}$ mice with less severe eye phenotype exhibit severe reduction of SOX2 protein in the lens and retina. High-magnification of dotted line areas in A, B, C, D are shown in A', B', C', D', respectively. (**E**) RT-qPCR analysis confirms significant *Sox2* downregulation in *Rbm24*$^{-/-}$ ocular tissue and (**F**) *rbm24a* morphant zebrafish. Abbr.: se, surface ectoderm; ov, optic vesicle; e, anterior epithelium of the lens; f, lens fiber cells; f.c., fold change. Asterisks in E and F indicate *P*-value < 0.05. Scale bar in A, B, C', D' is 70 µm, C-D is 140 µm, A', B' is 12 µm; # indicates whole embryonic tissue.

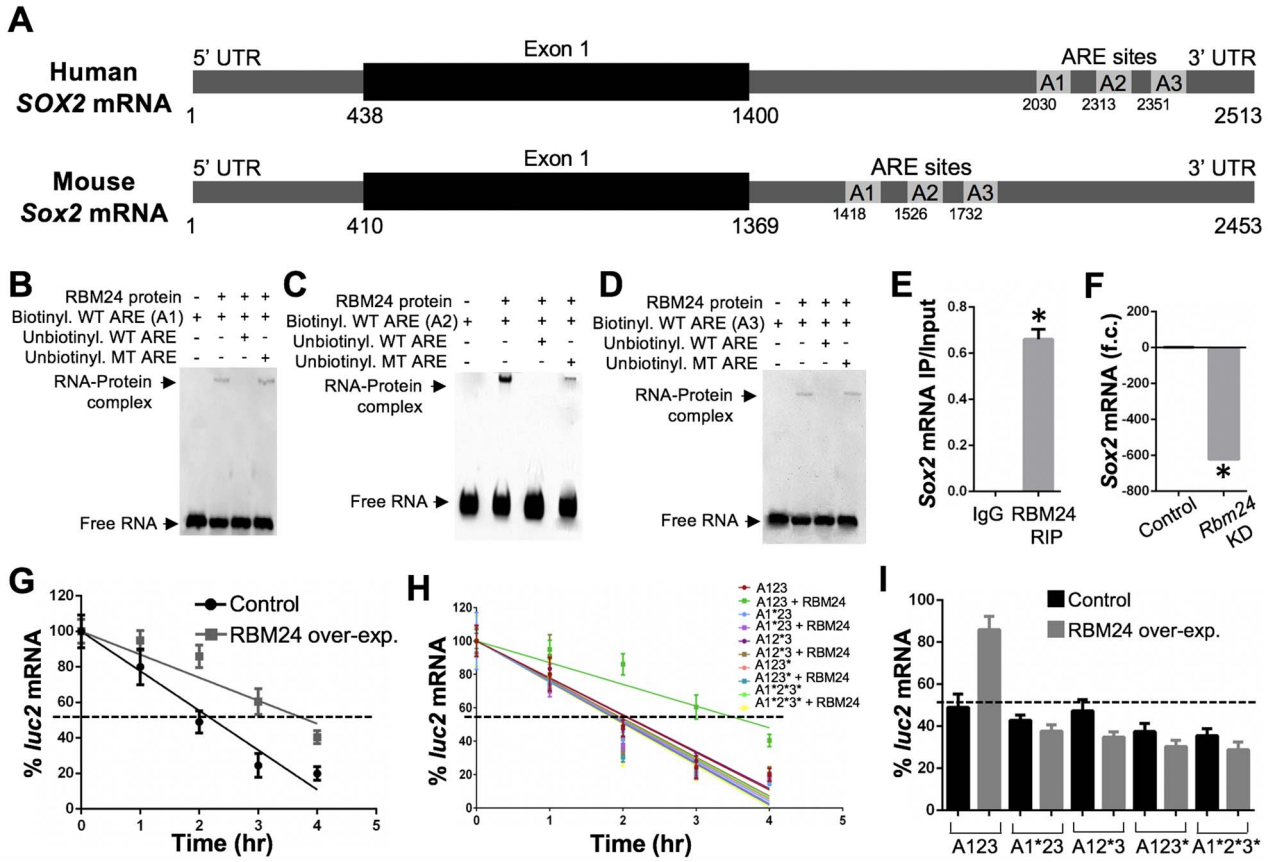

Figure 8. RBM24 regulates the half-life of Sox2 mRNA. (**A**) Schematic representation of human and mouse *SOX2* mRNA, which has a single exon and three AREs (A1, A2 and A3) in the 3'UTR. Relative positions of the human and mouse ARE sites are indicated. (**B-D**) RNA EMSA demonstrates that RBM24 protein binds to Sox2 3'UTR by directly interacting with its AU-rich element (A1-A3) to form a protein–RNA complex that can be competed away by un-labeled wild-type ARE containing oligomer but not by un-labeled mutant ARE. (**E**) RNA immunoprecipitation with RBM24 antibody on mouse embryonic eye tissue shows enrichment of *Sox2* mRNA. (**F**) *Rbm24* KD in NIH3T3 cells results in downregulation of *Sox2* transcript. (**G**) RBM24 overexpression in NIH3T3 cells results in significant increase in the half-life of luciferase mRNA fused to *Sox2* 3'UTR. (**H-I**) Upon RBM24 overexpression and actinomycin D treatment, *luciferase* reporter fused to wild-type *Sox2* 3'UTR mRNA exhibits elevated stability. However, under these conditions, the *luciferase* reporters fused to *Sox2* 3'UTR mRNA containing individual mutations in the AREs A1, A2 and A3 (*) or combined mutations in all three AREs (A1*2*3*) do not exhibit elevated stability. Luciferase mRNA levels after 2 h of actinomycin D treatment is shown as bar graph in I. Abbr.: IP, immunoprecipitate; ActD, actinomycin D; f.c., fold change. Asterisk in C indicates *P*-value < 0.05.

in the half-life of luciferase-*Sox2* reporter vector (Fig. 8H and I). These findings demonstrate that Rbm24 directly controls *Sox2* mRNA stability, which requires the presence of all three ARE sites in the Sox2 3'UTR.

Discussion

While signaling, transcriptional, epigenetic and non-coding RNA-mediated control of gene expression is well understood, the significance of RBP-mediated post-transcriptional control mechanisms in vertebrate organ development remains less clear. This represents a substantial knowledge gap considering that (1) RBPs are involved in every aspect of mRNA regulation such as capping, intracellular localization, stability/decay or translation (43), (2) there are similar number of RBPs encoded by the human genome as transcription factors (14–17) and (3) RBP function in RNA processing is increasingly recognized as a critical factor for understanding human disease phenotypes (15,44,45). Thus, our findings in this report have the following novelty and broad impact: (1) identification of SOX2 and LHX2 as a novel target of RBM24, (2) identification of an ARE-based mechanism for positively controlling Sox2 mRNA stability, (3) identification of RBM24 as the pioneering example of a conserved RBP that mediates post-transcriptional gene expression control necessary in vertebrate early eye development and (4) Rbm24 as a new gene linked to anophthalmia and microphthalmia eye defects. These data present a new model for defining the function of RBM24 in eye development (Fig. 9).

Previously, RBM24 has been linked to cardiac defects in vertebrates (24,25,46–49). In zebrafish, *rbm24a* and *rbm24b* knockdown results in craniofacial defects and microcephaly. While these studies also cursorily mention microphthalmia, the mechanism of these pathologies or the universal requirement of RBM24 in vertebrate eye development remained undefined. We show that in addition to the expression defects in key transcription factors, *Rbm24*$^{-/-}$ mice exhibit reduced *Birc2* and JAG1, which offers an explanation for the elevated apoptosis in these knockout mice as JAG1 downregulation is linked to increased apoptosis (40). Further, reduced SOX2 levels in *Rbm24*$^{-/-}$ mice also likely contribute to the increased cell death observed in the developing eye tissue, as SOX2 has been shown to negatively regulate apoptosis through the MAP4K4/survivin pathway in human lung cancer cells (50). In addition, misexpression of Pax6 in *Rbm24*$^{-/-}$ mice could result in downregulation of Pitx3 in the anterior region of the lens vesicle, which may impact apoptosis (51,52).

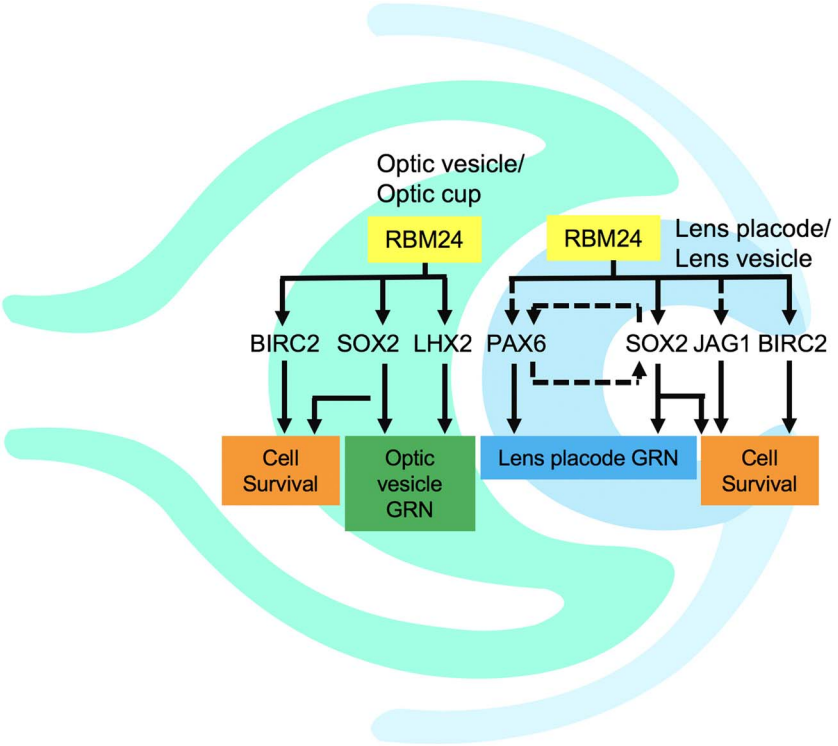

Figure 9. Model for RBM24-mediated post-transcriptional gene expression control in the early eye development. In normal eye development, RBM24 is required for positively regulating several key transcription factors in both the optic vesicle and the lens placode lineage. In the optic vesicle cells, RBM24 positively regulates LHX2 and SOX2 that in turn regulate the gene regulatory network of optic vesicle. In the lens placode, RBM24 regulates PAX6 and SOX2, thus regulating the gene regulatory network of the lens placode. Further it regulates JAG1 and BIRC2, which along with SOX2 regulates cell survival in both the lens and the retinal lineages.

In only one other context, in human mesenchymal stem cells, another RBP—HuR—has been shown to control SOX2 mRNA decay via the ARE sites, but even here, a direct interaction of the RBP–mRNA by EMSA is not described (53). But more importantly, the outcome of this HuR-based control results in the negative regulation of the Sox2 mRNA. In contrast, here we give the first evidence that RBM24 directly binds to the ARE sites of Sox2 mRNA 3'UTR and stabilizes it, perhaps by preventing the recruitment of RISC RNA decay complex to the mRNA by other RBPs such as HuR and thus protecting it from degradation. These findings inform on the complexity of combinatorial control mediated by distinct RBPs on the Sox2 mRNA and more generally on their exquisite specificity for key regulatory factors in development and disease. Moreover, the post-transcriptional control of SOX2 may represent an important regulatory mechanism as this gene is among the rare 3% genes encoded by just one exon (54) and thus the *Sox2* transcript—devoid of binding with proteins such as the exon–junction complex—may have evolved distinct mechanisms for controlling mRNA stability and half-life. Thus, we present a new molecular mechanism of RBM24-mediated post-transcriptional control of gene expression of the *Sox2* mRNA, which is required for proper development of the eye, and deficiency of which causes the ocular developmental defects anophthalmia and microphthalmia. Further, our new evidence of direct interactions between RBM24 and the ARE and the outcome of this interaction for the mRNA have broader impact, as 8% of mRNAs encoded by the human genome contain AREs in their 3'UTRs (55). Thus, these data point to new directions for investigating the relationship of Rbm24 with its target mRNAs in other cell and tissue types.

Finally, taken in the context of our recent discovery that the Tudor domain protein TDRD7 is linked to cataracts in human, mouse and chicken (29) and CELF1 is linked to cataract and/or lens defects in mouse, frog and zebrafish (31), these new findings on RBM24 firmly establish that post-transcriptional regulatory networks—like signaling and transcription networks—have evolved conserved functions to control eye development in vertebrates.

Materials and Methods

Animal husbandry

Mice used in this study were housed in the animal facility at the University of Delaware. The Institutional Animal Care and Use Committee (IACUC) at the University of Delaware approved animal experimental protocols, and all animal experiments were conducted in accordance with the Association for Research in Vision and Ophthalmology (ARVO) statement for the use of animals in ophthalmic and vision research (AUP#1226).

Generation of Rbm24-targeted deletion mouse mutants

A new conditional knockout mouse model was generated in this study wherein exon 1, 2 and 3 of *Rbm24* is flanked by *loxP* sites (*Rbm24*$^{flox/flox}$) (Genoway, Lyon, France). *Rbm24*$^{flox/flox}$ mice were crossed with *B6-Tg(CMV-Cre)1Cgn* mice carrying the *Cre* recombinase gene under the influence of the CMV promoter to generate constitutive knockout alleles of *Rbm24* (*Rbm24*$^{-/-}$). Embryos were staged by designating the day of observation of the vaginal plug as E0.5. Genotyping was performed on tail DNA prepared from post-natal or embryonic tissue using the Direct PCR Lysis reagent (Viagen Biotech, Los Angeles, CA). Animals were genotyped by using the following primers. *Rbm24* germline deletion allele is

amplified by primers: 5'-CAAGGACAGCCTGGGATACACAATACC-3′ and 5'-GCTATGTCCATCTTGGTTCAGGATTCAG-3′.

Zebrafish maintenance

All work involving zebrafish was approved by the University of Iowa's IACUC, PHS Assurance No. A3021-01, under animal protocol No. 5091513. Zebrafish embryos were raised between 28.5 and 30°C with no more than 50 embryos per 100 mm plate.

Knockdown of rbm24a in zebrafish by morpholinos

Zebrafish embryos collected from natural mating were pressure-injected at the 1–4 cell stage with 1–3 nanogram/embryo of translation blocking morpholino with the following sequence: *rbm24a*, 5′-GCATCCTCACGAAACGCTCAAGTGC-3′ (Gene Tools LLC, Philomath, OR). Standard control MO (5′-CCTCTTACCTCAGTTACAATT TATA-3′) was injected to generate 'control' zebrafish at an equal quantity as the experimental MO for each experiment. Microinjection volume was measured in a 1 µl capillary tube and calculated using the Microinjection Calculator Android app (available from Google Play Store).

CRISPR/Cas9 gene targeting

A vector containing the coding sequence for Cas9 protein flanked by two nuclear localization signals (nls) (pT3TS) was used to generate nls-Cas9-nls mRNA (56). Two sgRNAs were designed and constructed to target 20 bp sequences starting with guanine and preceding the PAM motif (5′-NGG-3′) to create a 252 bp deletion in *rbm24a* (57). Potential off-target effects of sgRNA candidates were analyzed using the online tool CRISPR Design developed by the Zhang laboratory (http://crispr.mit.edu/). An injection mixture was made containing 300 ng/µl Cas9 mRNA, 12.5 ng/µl of each guide RNA 5'-TAATACGACTCACTATAGGGGGAGATTGAAGAAGCTGGTTTTAGA GCTAGAA-3′ and 5'-TAATACGACTCACTATAGGCCTTCATGCAACC AAGTGGTTTTAGAGCTAGAA-3′.

ISH

Total RNA was isolated from 20 2-dpf zebrafish embryos. This total RNA was reverse transcribed into cDNA using SMART MMLV Reverse Transcriptase (Clontech) primed with oligo-dT primers. cDNA obtained was then used to clone a portion of *rbm24a* and *rbm24b* using the following primers: rbm24a-Forward-5'-CCAGGGGTTATGGATTTGTG-3′, rbm24a-Reverse-5'-TGCAGTTGTTGGGGTTGATA-3′, rbm24b-Forward-5'-CGGAGGTCTTCCCTATCACA-3′ and rbm24b-Reverse-5'-CCAAAC GCACACAAGAGCTA-3′. The products were ligated into a TOPO-TA PCR-II vector (Thermo Fisher Scientific, # K461020) following the manufacturers protocol. DIG-labeled RNA probes (DIG labeling Mix, Roche, #11277073910) were synthesized using T7 and SP6 Maxiscript kits (Thermo Fisher Scientific, #AM1320) following the manufacturers protocol. Embryos at 20 hpf and 2 dpf were fixed with 4% PFA, and ISH was performed as described previously (58,59). Post ISH, embryos underwent cryoprotection by sequential transfer from 1X PBST, to 15, 30% sucrose, then to OCT (optimal cutting temperature) embedding medium overnight. The following day, embryos were placed in blocks containing fresh OCT, aligned as desired and frozen. 8 µm sections were collected and imaged.

Western blot

Whole-body tissue from control (*Rbm24*$^{+/+}$) and *Rbm24*$^{-/-}$ mice at E14.5 was collected and lysed in RIPA buffer on ice. Western blot was performed as described previously (30) and probed with RBM24 antibody (diluted 1:200 in 5% milk in TBST) (Abcam, #ab174919) or beta-actin antibody (diluted 1:500 in 5% milk in TBST) (Abcam, #ab8227).

Immunofluorescence

Mouse head tissue from control (*Rbm24*$^{+/+}$) and *Rbm24*$^{-/-}$ mice at developmental stages E9.5, E10.5, E12.5 and E14.5 were flash frozen in OCT (Tissuetech, # 14-373-65). Frozen sections (16 µm thickness) were fixed with 4% PFA for 15 min at room temperature followed by three 1X PBS washes for 10 min each. The sections were then blocked in either 5% chicken serum (Abcam, # ab7477) or 10% BSA (Sigma-Aldrich, A2153) along with 0.3% Triton X-100 for 1 h at room temperature. NIH3T3 cells were fixed at 70% confluency with methanol for 10 min. The following primary antibodies were used in the given dilutions in the respective blocking buffers: RBM24 (Abcam, #ab94567, 1:100), SOX2 (EMD Millipore, #AB5603, 1:100), LHX2 (Santa Cruz Biotechnology, #sc-19 344, 1:100), SOX2 (Thermo Fisher Scientific, #48-1400, 1:200), OCT4 (Thermo Fisher Scientific, #PA5-27438, 1:200), PAX6 (EMD Millipore, #AB2237, 1:200), JAG1 (Santa Cruz Biotechnology, #sc8303, 1:50), E-cad (Cell Signaling Technology, #3195S, 1:100) and gamma-crystallin (Santa Cruz Biotechnology, # sc-22 415, 1:100). After 1-h blocking, the sections were incubated with the primary antibody overnight at 4°C. Slides were washed and incubated with the appropriate secondary antibody conjugated to Alexa Fluor 488 or 594 (Life Technologies, 1:200) and the nuclear stain DAPI (Thermo Fisher Scientific, #D21490, 1:1000). Slides were imaged using the Zeiss LSM 780 confocal microscope (Carl Zeiss Inc.).

Dark-field microscopy

Control (*Rbm24*$^{+/+}$) and *Rbm24*$^{-/-}$ mouse embryos at stage E11.5 were dissected in 1X PBS and imaged by light microscopy (Zeiss Stemi SV dissecting microscope).

RNA isolation and RT-qPCR in mouse

Rbm24$^{-/-}$ and *Rbm24*$^{+/+}$ ocular tissue at E14.5 was microdissected in 1X PBS for RNA isolation and flash frozen on dry ice and stored in −80°C until RNA isolation. Four E14.5 eyes were treated as one biological replicate, and total RNA was extracted from three biological replicates. Total RNA was extracted using RNeasy Mini Kit (Qiagen, #74104) with no modifications. On-column DNase treatment was performed using RNase-Free DNase (Qiagen, # 79254). RNA concentration was determined by using ND-1000 UV/Vis Spectrophotometer (NanoDrop Technologies; Software V3.8.1), and RNA was stored at −80°C until ready to use. cDNA synthesis was performed with 200 ng of RNA per reaction using manufacturer's instructions, and RT-qPCR was performed as described (32) on ABI7300 Real-Time PCR system (Applied Biosystems) using Fast SYBR Green PCR master mix by the investigator's laboratory (Invitrogen Life Technologies, # 4367659). *Hprt* was used as a control housekeeping gene to normalize transcript levels. The experiment was performed three times with three biological replicates. Differential expression of each transcript was determined using $2^{-\Delta\Delta CT}$ method. Statistical significance

for RT-qPCR data was determined using nested ANOVA (60). The following primers were used for qRT-PCR, Rbm24-Forward-5′-TCTTCGGAGACATCGAGGAA-3′ and Rbm24-Reverse-5′- AAAACCTGGCTGCATGATTC-3′, amplicon length, 200; Sox2-Forward-5′-TTAACGCAAAAACCGTGATG-3′ and Sox2-Reverse-5′-GAAGCGCCTAACGTACCACT-3′, amplicon length, 194; Jag1-Forward-5′-TAGCTGCCTGCCGAACCCCT-3′ and Jag1-Reverse-5′-GCTGGAGGCTGGAGGACCGA-3′, amplicon length, 590; and Pax6-Forward-5′- AGTTCTTCGCAACCTGGCTA-3′ and Pax6-Reverse-5′-ACTTGGACGGGAACTGACAC-3′, amplicon length, 846.

RNA isolation and RT-qPCR in zebrafish

RNA was isolated from 20 control (injected with control morpholino) and 20 *rbm24a* knockdown 1 dpf zebrafish embryos per biological replicate and used to synthesize cDNA as described above. Samples were prepared in a 96-well reaction plate with four biological replicates. qRT-PCR was performed with the LightCycler 480 System (Roche Applied Science) using SYBR Green I master mix (Roche, # 04707516001). Samples were normalized to *elongation factor 1 alpha* (*elfa*). Log fold change was determined using $2^{-\Delta\Delta CT}$, method and statistical significance was calculated using nested ANOVA. The following primers were used for RT-qPCR: sox2-Forward-5'-AACCAGAAAAACAGCCCGGA-3′, sox2-Reverse-5′-AATGGTCGCTTCTCGCTCTC-3′, elfa-Forward-5′-GATGCACCACGAGTCTCTGA-3′ and elfa-Reverse-5′-TGATGACCT GAGCGTTGAAG-3′.

RNA immunoprecipitation

Wild-type E14.5 mouse eye lysates were used ($n = 6$ eyes per biological replicate; total three biological replicates) for preconjugation with Rbm24 antibody (Abcam, #ab174919) and IgG with magnetic beads. Manufacturer's instructions were followed for the EZ-Nuclear RIP Kit (EMD Millipore, #17-10 523) for the immunoprecipitation, followed by cDNA synthesis and qRT-PCR for *Sox2* and *Hprt*.

RNA EMSA

Full-length *Rbm24* CDS fused with GST was cloned in PGEX-6P3 vector (GE Healthcare Life Sciences, #28-9546-51) and transformed in competent BL21 bacterial cells (Thermo Fisher Scientific, #C600003). Glutathione Sepharose bead (Sigma-Aldrich, #GE17-0756-01) was used to affinity purify Rbm24 protein from BL21 lysate, following which GST was cleaved from the fused protein using PreScissionTM Protease (GE Healthcare Life Sciences, #27-0843-01). RNA EMSA was performed using manufacturer's instruction for Chemiluminescent RNA EMSA (Thermo Fisher Scientific, #20158). A1 of *Sox2* 3′UTR were heated at 80°C for 5 min to relax RNA folding. Following RNA oligos were used: ARE1, 5′-ATTTGAACATTTTAGTTTTA-3′-biotin, 5′-ATTTGAACATTTTAGTTTTA-3′, 5′-ATTTGAACAGGGGAGTTTTA-3′-biotin; ARE2, 5′-ATTGTGATATTTTAAGGTTT-3′-biotin, 5′-ATTGTGATATTTTAAGGTTT-3′, 5′-ATTGTGATAGGGGAAGGTTT-3′-biotin; ARE3, 5′-TAGTTGTATTTTAAAAGATT-3′-biotin, 5′-TAGTTGTATTTTAAAAGATT-3′ and 5′-TAGTTGTAGGGGAAAAGAT T-3′. Rbm24 purified protein (0.5 mg/ml) was allowed to bind to the relaxed oligo for 30 min at room temperature. The samples were run on a 6% native gel polyacrylamide gel made in 0.5X TBE and then transferred to a nylon membrane. RNA was crosslinked to the membrane by irradiating the membrane with 254 nm UV lamp for 3 min. The membrane was then blocked; washed and biotinylated RNA was detected with chemiluminescent substrate provided in the kit.

TUNEL assay

The *in situ* cell death kit (Roche, #11684795910) was used for labeling cells undergoing apoptosis following the manufacturer instructions. The percent of TUNEL-positive nuclei was calculated as the ratio of TUNEL-positive nuclei and all nuclei multiplied by a factor of 100 (61,62). Apoptotic index was calculated from three biological replicates and three technical replicates.

Cell culture

The mouse fibroblast NIH3T3 cells and lens epithelial cell line 21EM15 were cultured under standard conditions (10 ml of DMEM with 4.5 g/l glucose and L-glutamine (Corning Cellgro, #10-017-CV)), 10% Fetal Bovine Serum (Gemini Bio Products, # 900-208) and 1% Penicillin-Streptomycin (GE Healthcare Life Sciences, # SV30010)). Cells were incubated at 37°C in a humid chamber with 5% CO2 as described previously (29,63).

Generation of Sox2 3′UTR reporter vector

To generate wild-type Sox2 reporter vector wherein *Renilla luciferase* is fused to 3′UTR of *Sox2* mRNA, wild-type Sox2 3′UTR was cloned downstream of the firefly luciferase gene in the pmirGLO vector (Promega, #E1330) with the following primers: 5′-GACGAGCTCGGGCTGGACTGCGAACTGGAGA-3′ and 5′-AGGCTCTAGATTCAGTGTCCATATTTCAAA-3′. Mutated Sox2 reporter vector were generated following manufacturer's instructions for QuikChange II Site-Directed Mutagenesis Kit (Agilent Technologies, #200523) using the below mentioned HPLC-purified primers: A1∗-Forward-5′-TGTTTTCCTTTTGTACA ATTTTAAAACTCCCCTGTTCAAATCCGAATAAACTCCTTCCTTGT TTGTAACGG-3′, A1∗-Reverse-5′- CCGTTACAAACAAGGAAGGAGT TTATTCGGATTTGAACAGGGGAGTTTTAAAATTGTACAAAAGGAA AACA-3′, A2∗-Forward-5′-GAAATATTTTCTTATGGTTTGTAATATT TCTGTAAATTGTGATACCCCAAGGTTTTTCCCCCCTTTTATTTTCC G-3′, A2∗-Reverse-5′-CGGAAAATAAAAGGGGGGAAAAACCTTGG GGTATCACAATTTACAGAAATATTACAAACCATAAGAAAATATTTC-3′, A3∗-Forward-5′-CTGATTCCAATAACAGAGCCGAATCTTTTGGG GTACAACTACGGAAAATAAAAGGGGGGAAA-3′ and A3∗-Reverse-5′-TTTCCCCCCTTTTATTTTCCGTAGTTGTACCCCAAAAGATTCGG CTCTGTTATTGGAATCAG-3′. pmirGLO dual luciferase vector with wild-type 3′UTR of Sox2 vector was used as a template for site-directed mutagenesis. Cloning was confirmed by Sanger sequencing.

mRNA decay assay

To generate the RBM24 overexpression plasmid, RBM24 ORF was cloned to pcDNA3.1 vector (Thermo Fisher Scientific, # V79020) using the following primers, Forward-5′-ATTAGAATTCATGCACA CCACCCAGAA-3′ and Reverse-5′- CTTCTCGAGCTACTGCATTCGG TCTGTCT-3′, and was confirmed by Sanger sequencing. For *Lhx2* decay assays, RBM24 overexpression vector was transiently transfected into 21EM15 cells for 48 h using the Lipofectamine® 3000 Transfection Reagent (Thermo Fisher Scientific, #L3000015). Control cells were transfected with empty pcDNA3.1 vector. Transfected cells were treated with 5 μg/ml actinomycin D to halt general transcription. Cells were collected every 2 h up to

after 10 h of actinomycin D treatment, total RNA was isolated and cDNA were synthesized, and RT-qPCRs were performed as described above. For *Sox2* decay assays, both RBM24 overexpression plasmid and the dual luciferase-Sox2 3'UTR plasmid were transiently transfected into NIH3T3 cells for 48 h using the Lipofectamine® 3000 Transfection Reagent (Thermo Fisher Scientific, #L3000015). Control cells were transfected with empty pcDNA3.1 vector and dual luciferase-Sox2 3'UTR plasmid. Transfected cells were treated with 5 μg/ml actinomycin D to halt general transcription. Cells were collected every hour up to after 4 h of actinomycin D treatment, total RNA was isolated and cDNA were synthesized, and RT-qPCRs were performed as described above using the following primers to amplify the luciferase product: 5′-GCTCAGCAAGGAGGTAGGTG-3′ and 5′- TCTTACCGGTGTCCAAGTCC-3′. The assay was performed multiple times with three biological replicates and three technical replicates.

Funding

This work was supported by National Institutes of Health's National Eye Institute [grant number R01EY029770 to S.L.]. Support from the University of Delaware Core Imaging facility was made possible through the Institutional Development Award (IDeA) from the National Institutes of Health's National Institute of General Medical Sciences INBRE Program Grant [grant number P20GM103446]. Acquisition of the confocal microscope used in this study was funded by the National Institutes of Health/National Center for Research Resources grant [1S10 RR027273]. S.D. received a Summer Scholarship from Fight For Sight, Inc. S.L. is a Pew Scholar in the Biomedical Sciences.

Conflict of interest statement

None declared.

References

1. Danno, H., Michiue, T., Hitachi, K., Yukita, A., Ishiura, S. and Asashima, M. (2008) Molecular links among the causative genes for ocular malformation: Otx2 and Sox2 coregulate Rax expression. *Proc. Natl. Acad. Sci. U. S. A.*, **105**, 5408–5413.
2. Chow, R.L. and Lang, R.A. (2001) Early eye development in vertebrates. *Annu. Rev. Cell Dev. Biol.*, **17**, 255–296.
3. Zuber, M.E., Gestri, G., Viczian, A.S., Barsacchi, G. and Harris, W.A. (2003) Specification of the vertebrate eye by a network of eye field transcription factors. *Development*, **130**, 5155–5167.
4. Chiang, C., Litingtung, Y., Lee, E., Young, K.E., Corden, J.L., Westphal, H. and Beachy, P.A. (1996) Cyclopia and defective axial patterning in mice lacking sonic hedgehog gene function. *Nature*, **383**, 407–413.
5. Shah, S.P., Taylor, A.E., Sowden, J.C., Ragge, N.K., Russell-Eggitt, I., Rahi, J.S. and Gilbert, C.E. (2011) Anophthalmos, microphthalmos, and typical coloboma in the United Kingdom: a prospective study of incidence and risk. *Invest. Ophthalmol. Vis. Sci.*, **52**, 558–564.
6. Reis, L.M. and Semina, E.V. (2015) Conserved genetic pathways associated with microphthalmia, anophthalmia, and coloboma. *Birth Defects Res. C Embryo Today*, **105**, 96–113.
7. Kamachi, Y., Sockanathan, S., Liu, Q., Breitman, M., Lovell-Badge, R. and Kondoh, H. (1995) Involvement of SOX proteins in lens-specific activation of crystallin genes. *EMBO J.*, **14**, 3510–3519.
8. Taranova, O.V., Magness, S.T., Fagan, B.M., Wu, Y., Surzenko, N., Hutton, S.R. and Pevny, L.H. (2006) SOX2 is a dose-dependent regulator of retinal neural progenitor competence. *Genes Dev.*, **20**, 1187–1202.
9. Fantes, J., Ragge, N.K., Lynch, S.-A., McGill, N.I., Collin, J.R.O., Howard-Peebles, P.N., Hayward, C., Vivian, A.J., Williamson, K., van Heyningen, V. *et al.* (2003) Mutations in SOX2 cause anophthalmia. *Nat. Genet.*, **33**, 461–463.
10. Williamson, K.A. and FitzPatrick, D.R. (2014) The genetic architecture of microphthalmia, anophthalmia and coloboma. *Eur. J. Med. Genet.*, **57**, 369–380.
11. Takahashi, K. and Yamanaka, S. (2006) Induction of pluripotent stem cells from mouse embryonic and adult fibroblast cultures by defined factors. *Cell*, **126**, 663–676.
12. Takahashi, K., Tanabe, K., Ohnuki, M., Narita, M., Ichisaka, T., Tomoda, K. and Yamanaka, S. (2007) Induction of pluripotent stem cells from adult human fibroblasts by defined factors. *Cell*, **131**, 861–872.
13. Wu, J. and Belmonte, J.C.I. (2016) The molecular harbingers of early mammalian embryo patterning. *Cell*, **165**, 13–15.
14. Gerstberger, S., Hafner, M. and Tuschl, T. (2014) A census of human RNA-binding proteins. *Nat. Rev. Genet.*, **15**, 829–845.
15. Hentze, M.W., Castello, A., Schwarzl, T. and Preiss, T. (2018) A brave new world of RNA-binding proteins. *Nat. Rev. Mol. Cell Biol.*, **19**, 327–341.
16. Vaquerizas, J.M., Kummerfeld, S.K., Teichmann, S.A. and Luscombe, N.M. (2009) A census of human transcription factors: function, expression and evolution. *Nat. Rev. Genet.*, **10**, 252–263.
17. Lambert, S.A., Jolma, A., Campitelli, L.F., Das, P.K., Yin, Y., Albu, M., Chen, X., Taipale, J., Hughes, T.R. and Weirauch, M.T. (2018) The human transcription factors. *Cell*, **172**, 650–665.
18. Kakrana, A., Yang, A., Anand, D., Djordjevic, D., Ramachandruni, D., Singh, A., Huang, H., Ho, J.W.K. and Lachke, S.A. (2018) iSyTE 2.0: a database for expression-based gene discovery in the eye. *Nucleic Acids Res.*, **46**, D875–D885.
19. Anand, D., Kakrana, A., Siddam, A.D., Motohashi, H., Yamamoto, M. and Lachke, S.A. (2018) RNA sequencing-based transcriptomic profiles of embryonic lens development for cataract gene discovery. *Hum. Genet.*, **137**, 941–954.
20. Lachke, S.A., Ho, J.W.K., Kryukov, G.V., O'Connell, D.J., Aboukhalil, A., Bulyk, M.L., Park, P.J. and Maas, R.L. (2012) iSyTE: integrated systems tool for eye gene discovery. *Invest. Ophthalmol. Vis. Sci.*, **53**, 1617–1627.
21. Fetka, I., Radeghieri, A. and Bouwmeester, T. (2000) Expression of the RNA recognition motif-containing protein SEB-4 during Xenopus embryonic development. *Mech. Dev.*, **94**, 283–286.
22. Grifone, R., Xie, X., Bourgeois, A., Saquet, A., Duprez, D. and Shi, D. (2014) The RNA-binding protein Rbm24 is transiently expressed in myoblasts and is required for myogenic differentiation during vertebrate development. *Mech. Dev.*, **134**, 1–15.
23. Yang, J., Hung, L.-H., Licht, T., Kostin, S., Looso, M., Khrameeva, E., Bindereif, A., Schneider, A. and Braun, T. (2014) RBM24 is a major regulator of muscle-specific alternative splicing. *Dev. Cell*, **31**, 87–99.
24. Zhang, T., Lin, Y., Liu, J., Zhang, Z.G., Fu, W., Guo, L.Y., Pan, L., Kong, X., Zhang, M.K., Lu, Y.H. *et al.* (2016) Rbm24 regulates

alternative splicing switch in embryonic stem cell cardiac lineage differentiation. *Stem Cells*, **34**, 1776–1789.
25. Liu, J., Kong, X., Zhang, M., Yang, X. and Xu, X. (2019) RNA binding protein 24 deletion disrupts global alternative splicing and causes dilated cardiomyopathy. *Protein Cell*, **10**, 405–416.
26. Jiang, Y., Zhang, M., Qian, Y., Xu, E., Zhang, J. and Chen, X. (2014) Rbm24, an RNA-binding protein and a target of p53, regulates p21 expression via mRNA stability. *J. Biol. Chem.*, **289**, 3164–3175.
27. Xu, E., Zhang, J., Zhang, M., Jiang, Y., Cho, S. and Chen, X. (2014) RNA-binding protein RBM24 regulates p63 expression via mRNA stability. *Mol. Cancer Res.*, **12**, 359–369.
28. Zhang, M., Zhang, Y., Xu, E., Mohibi, S., de Anda, D.M., Jiang, Y., Zhang, J. and Chen, X. (2018) Rbm24, a target of p53, is necessary for proper expression of p53 and heart development. *Cell Death Differ.*, **25**, 1118–1130.
29. Lachke, S.A., Alkuraya, F.S., Kneeland, S.C., Ohn, T., Aboukhalil, A., Howell, G.R., Saadi, I., Cavallesco, R., Yue, Y., Tsai, A.C.-H. *et al.* (2011) Mutations in the RNA granule component TDRD7 cause cataract and glaucoma. *Science*, **331**, 1571–1576.
30. Dash, S., Dang, C.A., Beebe, D.C. and Lachke, S.A. (2015) Deficiency of the RNA binding protein caprin2 causes lens defects and features of peters anomaly. *Dev. Dyn.*, **244**, 1313–1327.
31. Siddam, A.D., Gautier-Courteille, C., Perez-Campos, L., Anand, D., Kakrana, A., Dang, C.A., Legagneux, V., Méreau, A., Viet, J., Gross, J.M. *et al.* (2018) The RNA-binding protein Celf1 post-transcriptionally regulates p27Kip1 and Dnase2b to control fiber cell nuclear degradation in lens development. *PLoS Genet.*, **14**, e1007278.
32. Agrawal, S.A., Anand, D., Siddam, A.D., Kakrana, A., Dash, S., Scheiblin, D.A., Dang, C.A., Terrell, A.M., Waters, S.M., Singh, A. *et al.* (2015) Compound mouse mutants of bZIP transcription factors Mafg and Mafk reveal a regulatory network of non-crystallin genes associated with cataract. *Hum. Genet.*, **134**, 717–735.
33. Grifone, R., Saquet, A., Xu, Z. and Shi, D. (2018) Expression patterns of Rbm24 in lens, nasal epithelium, and inner ear during mouse embryonic development. *Dev. Dyn.*, **247**, 1160–1169.
34. Wagner, D.E., Weinreb, C., Collins, Z.M., Briggs, J.A., Megason, S.G. and Klein, A.M. (2018) Single-cell mapping of gene expression landscapes and lineage in the zebrafish embryo. *Science*, **360**, 981–987.
35. Brastrom, L.K., Scott, C.A., Dawson, D.V. and Slusarski, D.C. (2019) A high-throughput assay for congenital and age-related eye diseases in Zebrafish. *Biomedicine*, **7**, 28.
36. French, C.R., Stach, T.R., March, L.D., Lehmann, O.J. and Waskiewicz, A.J. (2013) Apoptotic and proliferative defects characterize ocular development in a microphthalmic BMP model. *Invest. Ophthalmol. Vis. Sci.*, **54**, 4636–4647.
37. den Hollander, A.I., Biyanwila, J., Kovach, P., Bardakjian, T., Traboulsi, E.I., Ragge, N.K., Schneider, A. and Malicki, J. (2010) Genetic defects of GDF6 in the zebrafish out of sight mutant and in human eye developmental anomalies. *BMC Genet.*, **11**, 102.
38. Silver, J. and Hughes, A.F.W. (1974) The relationship between morphogenetic cell death and the development of congenital anophthalmia. *J. Comp. Neurol.*, **157**, 281–301.
39. Le, T.T., Conley, K.W., Mead, T.J., Rowan, S., Yutzey, K.E. and Brown, N.L. (2012) Requirements for Jag1-Rbpj mediated Notch signaling during early mouse lens development. *Dev. Dyn.*, **241**, 493–504.
40. Fiaschetti, G., Schroeder, C., Castelletti, D., Arcaro, A., Westermann, F., Baumgartner, M., Shalaby, T. and Grotzer, M.A. (2014) NOTCH ligands JAG1 and JAG2 as critical pro-survival factors in childhood medulloblastoma. *Acta Neuropathol. Commun.*, **2**, 39.
41. Osathanon, T., Nowwarote, N., Pavasant, P. and Waleerat, S. (2015) Influence of Jagged1 on apoptosis-related gene expression: a microarray database analysis. *Genes Genom.*, **37**, 837–843.
42. Smith, A.N., Miller, L.-A., Radice, G., Ashery-Padan, R. and Lang, R.A. (2009) Stage-dependent modes of Pax6-Sox2 epistasis regulate lens development and eye morphogenesis. *Development*, **136**, 2977–2985.
43. Dash, S., Siddam, A.D., Barnum, C.E., Janga, S.C. and Lachke, S.A. (2016) RNA binding proteins in eye development and disease: implication of conserved RNA granule components. *Wiley Interdiscip. Rev. RNA*, **7**, 527–557.
44. Manning, K.S. and Cooper, T.A. (2017) The roles of RNA processing in translating genotype to phenotype. *Nat. Rev. Mol. Cell Biol.*, **18**, 102–114.
45. Turner, M. and Díaz-Muñoz, M.D. (2018) RNA-binding proteins control gene expression and cell fate in the immune system. *Nat. Immunol.*, **19**, 120–129.
46. Li, H.-Y., Bourdelas, A., Carron, C. and Shi, D.L. (2010) The RNA-binding protein Seb4/RBM24 is a direct target of MyoD and is required for myogenesis during Xenopus early development. *Mech. Dev.*, **127**, 281–291.
47. Poon, K.L., Tan, K.T., Wei, Y.Y., Ng, C.P., Colman, A., Korzh, V. and Xu, X.Q. (2012) RNA-binding protein RBM24 is required for sarcomere assembly and heart contractility. *Cardiovasc. Res.*, **94**, 418–427.
48. van den Hoogenhof, M.M.G., van der Made, I., de Groot, N.E., Damanafshan, A., van Amersfoorth, S.C.M., Zentilin, L., Giacca, M., Pinto, Y.M. and Creemers, E.E. (2018) AAV9-mediated Rbm24 overexpression induces fibrosis in the mouse heart. *Sci. Rep.*, **8**, 11696.
49. Maragh, S., Miller, R.A., Bessling, S.L., Wang, G., Hook, P.W. and McCallion, A.S. (2014) Rbm24a and Rbm24b are required for normal somitogenesis. *PLoS One*, **9**, e105460.
50. Chen, S., Li, X., Lu, D., Xu, Y., Mou, W., Wang, L., Chen, Y., Liu, Y., Li, X., Li, L. *et al.* (2014) SOX2 regulates apoptosis through MAP4K4-survivin signaling pathway in human lung cancer cells. *Carcinogenesis*, **35**, 613–623.
51. Chauhan, B.K., Reed, N.A., Zhang, W., Duncan, M.K., Kilimann, M.W. and Cvekl, A. (2002) Identification of genes downstream of Pax6 in the mouse lens using cDNA microarrays. *J. Biol. Chem.*, **277**, 11539–11548.
52. Medina-Martinez, O., Shah, R. and Jamrich, M. (2009) Pitx3 controls multiple aspects of lens development. *Dev. Dyn.*, **238**, 2193–2201.
53. Latorre, E., Carelli, S., Caremoli, F., Giallongo, T., Colli, M., Canazza, A., Provenzani, A., Di Giulio, A.M. and Gorio, A. (2016) Human antigen R binding and regulation of SOX2 mRNA in human Mesenchymal stem cells. *Mol. Pharmacol.*, **89**, 243–252.
54. Grzybowska, E.A. (2012) Human intronless genes: functional groups, associated diseases, evolution, and mRNA processing in absence of splicing. *Biochem. Biophys. Res. Commun.*, **424**, 1–6.
55. Bakheet, T., Hitti, E. and Khabar, K.S.A. (2018) ARED-plus: an updated and expanded database of AU-rich

element-containing mRNAs and pre-mRNAs. *Nucleic Acids Res.*, **46**, D218–D220.
56. Hwang, W.Y., Fu, Y., Reyon, D., Maeder, M.L., Kaini, P., Sander, J.D., Joung, J.K., Peterson, R.T. and Yeh, J.J. (2013) Heritable and precise zebrafish genome editing using a CRISPR-Cas system. *PLoS One*, **8**, e68708.
57. Fu, Y., Sander, J.D., Reyon, D., Cascio, V.M. and Joung, J.K. (2014) Improving CRISPR-Cas nuclease specificity using truncated guide RNAs. *Nat. Biotechnol.*, **32**, 279–284.
58. Thisse, C., Thisse, B., Schilling, T.F. and Postlethwait, J.H. (1993) Structure of the zebrafish snail1 gene and its expression in wild-type, spadetail and no tail mutant embryos. *Development*, **119**, 1203–1215.
59. Schneider, I., Houston, D.W., Rebagliati, M.R. and Slusarski, D.C. (2008) Calcium fluxes in dorsal forerunner cells antagonize beta-catenin and alter left-right patterning. *Development*, **135**, 75–84.
60. Bookout, A.L. and Mangelsdorf, D.J. (2003) Quantitative real-time PCR protocol for analysis of nuclear receptor signaling pathways. *Nucl. Recept. Signal.*, **1**, e012.
61. Ryu, J.-H., Kim, S.-H., Lee, H.-Y., Bai, J.Y., Nam, Y., Bae, J., Lee, D., Shin, S.C., Ha, E. and Lee, W. (2008) Innate immune homeostasis by the homeobox gene caudal and commensal-gut mutualism in drosophila. *Science*, **319**, 777–782.
62. Zahalka, A.H., Arnal-Estapé, A., Maryanovich, M., Nakahara, F., Cruz, C.D., Finley, L.W.S. and Frenette, P.S. (2017) Adrenergic nerves activate an angio-metabolic switch in prostate cancer. *Science*, **358**, 321–326.
63. Terrell, A.M., Anand, D., Smith, S.F., Dang, C.A., Waters, S.M., Pathania, M., Beebe, D.C. and Lachke, S.A. (2015) Molecular characterization of mouse lens epithelial cell lines and their suitability to study RNA granules and cataract associated genes. *Exp. Eye Res.*, **131**, 42–55.